IEEE Access
Multidisciplinary ⋮ Rapid Review ⋮ Open Access Journal

Received February 22, 2021, accepted March 1, 2021, date of publication March 15, 2021, date of current version March 25, 2021.

Digital Object Identifier 10.1109/ACCESS.2021.3065988

A Compact 8-Element 3D UWB Diversity Antenna System for Off Device Installation

SANIA SHAKIR[1], MUHAMMAD BILAL[1], SYED MUZAHIR ABBAS[2], (Senior Member, IEEE), NOMAN SALEEM[3], ZAHID RAUF[1], (Member, IEEE), RAJA ASIF WAGAN[1], RASHID SALEEM[4], AND MUHAMMAD FARHAN SHAFIQUE[5], (Senior Member, IEEE)

[1]Department of Telecommunication Engineering, Balochistan University of IT, Engineering and Management Sciences, Quetta 87300, Pakistan
[2]Faculty of Science and Engineering, School of Engineering, Macquarie University, Sydney, NSW 2109, Australia
[3]Chief Minister Delivery Unit, Chief Minister Secretariat, Quetta 87300, Pakistan
[4]Telecommunication Engineering Department, University of Engineering and Technology (UET) Taxila, Taxila 47050, Pakistan
[5]Center for Advanced Studies in Telecommunication, COMSATS University Islamabad, Islamabad 45550, Pakistan

Corresponding author: Sania Shakir (sania.shakir17@outlook.com)

ABSTRACT In this paper, an 8-element Ultra-wideband Multiple-Input-Multiple-Output (UWB-MIMO) antenna system is proposed. This MIMO system has novel miniaturized antenna elements that are evolved from a conventional monopole patch antenna. These antennas incorporate various impedance matching features including but are not limited to smoothly tapered fed lines, split and truncated ground configuration, semi-circles arches, and inverted p-shaped slots. The antenna pairs are arranged in the cuboidal form to achieve a 3D-arrangement whereas customized decoupling structures achieve the desired isolation levels for three configurations including side-by-side, orthogonal, and across. These three distinct isolation mechanism offers isolation ranges from 20–30 dB for the proposed configurations. More importantly, a diamond eye structure (DES) as a parasitic element is also designed and optimized to improve the impedance matching owing to the lossy nature of isolation structures. The proposed antenna system has compact dimensions of $26.9 \times 26 \times 26.9$ mm^3 and its investigated MIMO performance proves its suitability for communication devices operating in the whole UWB spectrum of 3.1–10.6 GHz.

INDEX TERMS Frequency selective surfaces (FSS), multiple-input-multiple-output (MIMO), mutual coupling, ultra-wideband (UWB) antennas.

I. INTRODUCTION

Wideband wireless technologies are imminent to catch up with the demands of current and future communication requirements. Acknowledging the fact, the Federal Communication Commission (FCC) has allowed the usage of an unlicensed spectrum of more than 7 GHz for Ultra Wide-band (UWB) applications. This band ranges from 3.1 GHz to 10.6 GHz [1]. In order to protect the existing frequency bands in this range, a power spectral density restriction of 41 dBm/MHz has been imposed. This UWB spectrum has gained huge attraction for its potential applications in remote sensing, radars, geo-location, medical imaging, and wireless communications [2], [3].

Although the bandwidth available is very large, the gigabit data rate is still very challenging to achieve owing to the limitation on power spectral density. Multiple Input Multiple Output (MIMO) systems are another exceptional technology that uses multiple antenna elements on both receiving and transmitting ends to enhance the data rate by exploiting the multipath characteristics of a channel [4].

MIMO and UWB technology together have shown some promising results for short-range high-speed communications like in Wireless Personal Area Network (WPAN) [5]. The diversity characteristics of UWB-MIMO technology have been investigated meticulously in the last decade by reporting various designs on spatial, pattern, and polarization diversity. The main challenge associated with spatial diversity techniques is the footprint of the antenna element since the radiating elements are physically separated to exploit multipath propagation hence compactness remains a problem [6].

In a recent research work reported in [7], a pair of eye-shaped monopole planar antennas with a T-shaped decoupling structure in the ground plane is proposed. The reported design achieves isolation of 20 dB with overall dimensions of 18×36 mm^2. In another study, a pair of circular shaped

The associate editor coordinating the review of this manuscript and approving it for publication was Lei Ge.

monopole antennas are presented [8]. The design achieves its decoupling through a Y shape stub on the rear side along with multi-section slits in the feeding lines. The design measuring 25 × 32 mm^2 offers a mutual coupling of less than 20 dB in the whole UWB band. Similarly, an orthogonally placed four-element UWB MIMO antenna is presented in [9]. The design incorporates a staircase-shaped decoupling mechanism along with multiple slits and slots to improve the isolation up to 22 dB with an overall size of 39 × 39 mm^2. A two-element planar monopole UWB MIMO antenna system has been proposed in [10] The design has sinusoidal slots and rectangular slits in the ground plane to achieve the desired isolation. The design is 30 × 50.5 mm^2 in size with an isolation level of above 20 dB in the whole band. In [11], a quad-port planar circular monopole antenna having rectangular shaped parasitic elements is placed orthogonally with an elliptical slotted square ground. This reported design achieves 20 dB isolation with much larger dimensions of 94.2 × 94.2 mm^2. In another article, a two-port semicircular monopole radiator with a fence-type decoupling structure has been reported in [12]. The decoupling structure contains 16 slits and an L-shaped parasitic structure introduced in the ground plane. The design offers isolation of 20 dB in the whole band with dimensions of 50 × 35 mm^2. A dual-port UWB-MIMO Vivaldi antenna is reported in [13]. The reported design comprises four Split-Ring Resonators (SRRs) and a T-shaped slot etches in the ground plane to achieve limited isolation of 16 dB whilst having dimensions of 26 × 26 mm^2. In [14], a planar quad element circular polarized UWB antenna system has been proposed with a wide axial bandwidth. The decoupling is achieved by introducing protruding hexagonal stubs in the ground plane. The design provides 18 dB isolation with the dimensions of 45 × 45 mm^2. Likewise, four-port semi-elliptical self-complementary monopole radiators with modified grounds are reported in [15]. This design comprises L-shape slits and a Complementary Split Ring Resonator (CSRR) in the antenna radiator to attain band notching and isolation of 16 dB with comparatively larger dimensions of 63 × 63 mm^2.

Most of the literature available on UWB MIMO comprises planar designs. These designs are helpful in consumer electronics at receiving ends, however, in other scenarios where an off-device antenna mounting is possible it is best to use 3D antennas which can radiate in all directions hence ensuring best connectivity and highest data rates by maximum utilization of multipath effect in rich scattering indoor or outdoor environments. In this regards a few research papers have been proposed like in [16] a dual-port 3D MIMO antenna consisting of rectangular patches with an inverted U shape and an F shape decoupling elements are presented. The design provides isolation of 20 dB and a size of 40 × 36 mm^2. In [17], a dual-port tapered rectangular antenna with the modified ground is presented. This design makes the 3D structure by placing antennas in a side-by-side and back-to-back arrangement. Four C-shaped strips and three rectangular vertical stubs are introduced in the ground to improve isolation up to 20 dB with a size of 40 × 37.5 mm^2. Another dual-port 3D MIMO antenna having improved rectangular radiators are reported in [18]. The design comprises grid-like interdigital FSS structures with the modified ground to provide better isolation. The design consisted of a T-shaped slot etched from the radiator that improved impedance matching in both orthogonal and back-to-back arrangements and achieved the isolation of 20 dB with the dimensions of 40 × 35 mm^2.

In this paper, an eight-element non-planar UWB-MIMO antenna system is proposed. The antenna elements are mounted on a cubic polystyrene block and each of the four sides consists of an antenna pair having feeding ports in the opposite directions. Owing to 3D composition, the elements naturally develop high mutual coupling among side-by-side, orthogonal, and back-to-back or across elements. A decoupling structure having meander lines and spiral-shaped FSS has been proposed to minimize the mutual coupling. The decoupling mechanism offers more than 20 dB isolation over the whole band of UWB in all configurations. All MIMO performance parameters have been investigated and are found to be within acceptable limits.

The rest of the paper is organized as follows. In Section II, the geometrical configuration of the proposed antenna system, decoupling mechanism, and parasitic structure is discussed. Simulated and measured results including return loss, isolation, surface current distribution, radiation characteristics, and MIMO performance parameters are presented in Section III. A detailed discussion and comparison with the existing literature with the proposed system is presented in Section IV. Finally, Section V concludes the paper.

II. GEOMETRICAL CONFIGURATION

A. UWB MIMO ANTENNA CONFIGURATION

The proposed antenna pair is designed on a low cost 1.6 mm thick FR-4 substrate having dimensions of 26 × 26 mm^2. The employed laminate has a relative permittivity $\varepsilon_r = 4.4$ and dielectric loss tangent $\tan\delta = 0.02$. This antenna design comprises step-by-step evolution from circular monopole antennas to an optimized design incorporating Defected Ground Structures (DGS). The design evolution is summarized in 5 steps as shown in Fig. 1.

The MIMO geometry is evolved from a conventional circular monopole patch antenna with a square ground plane and rectangular feed line. These monopoles have a resonant response at 8 GHz with very limited bandwidth. The antenna bandwidth is improved by employing various bandwidth enhancement mechanisms in the following steps.

In the second step, the feed lines and radiators are modified by reshaping them, feed lines are made tapered at the feeding edge and the circular radiator is transformed into the mickey mouse shape geometry. This modification is necessary to improve the impedance matching at lower frequency bands which are caused by the larger physical area of the radiator.

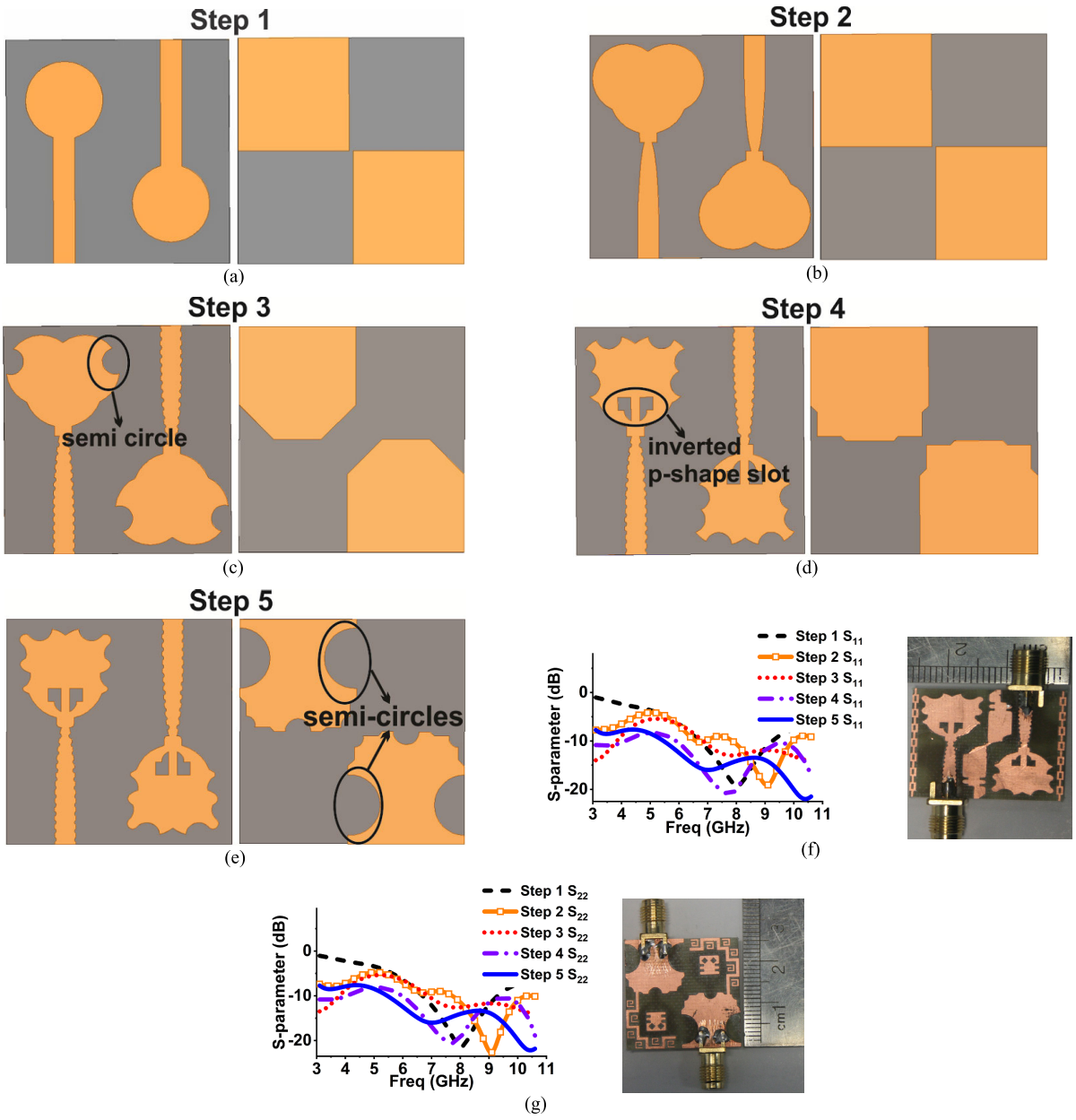

FIGURE 1. Step by step antenna configuration from step 1-5: (a)-(e) and antenna variations from step1-5 (f)S_{11} and (g) S_{22}.

In follow-up step 3, the radiators are further modified by etching semi-circles along their edges to introduce current perturbation. The ground plane is also chamfered on the top edges to enhance impedance bandwidth. These modifications further improve the performance at a lower frequency band. The feeding line is made zigzag to address the matching issues at the higher frequency spectrum.

The radiators offer optimum matching for lower and higher bands however the middle band around 7 GHz needs further improvement. Therefore an inverted P shape slots are introduced to the radiators near the feeding edge and triangles are added on top edges of the ground plane. This improves the impedance in the middle frequency band.

In the final variation, the ground plane is modified by further perturbing the current path by introducing various defects along the edges and also the radiator's sharp edges are smoothened to achieve better current flow over the antenna as shown in Fig 2 (e). All these changes ensemble help in achieving the desired impedance matching over the whole UWB band. The scattering parameters of these variations are shown in Fig 2(f) and (g).

B. DECOUPLING STRUCTURE CONFIGURATION

The design develops coupling in three sensitive areas, first one is the pair of antenna arranged side-by-side on a single substrate. There is a strong mutual coupling between these antennas and to suppress it, a vertical decoupling

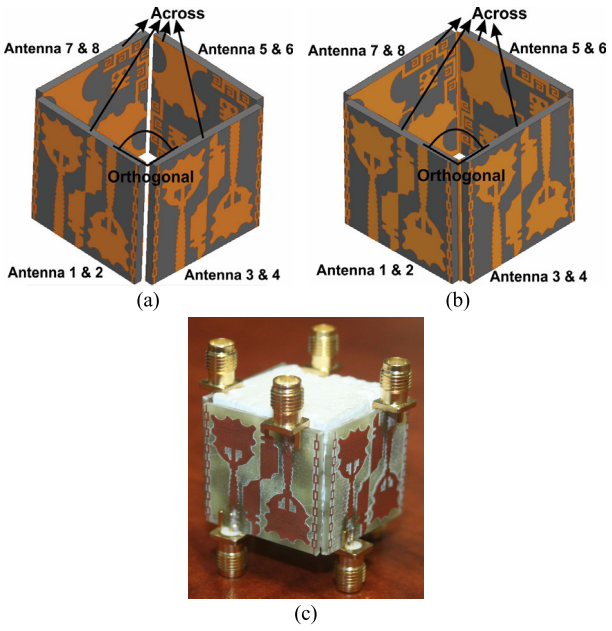

FIGURE 2. Compact antenna: (a) non SGP; (b) SGP and (c) fabricated view.

transmission line resonant structure is introduced. Initially, it was designed by employing a microstrip line calculated at middle frequency i.e. 6.5 GHz with characteristics impedance Z_0 =50Ω [19]. The initial approximated length and width $l_1 \times l_4$ are found to be (12.6 × 2) mm × 3.1 mm respectively. Region l_2 is then designed to join these lengths to make the vertical structure between side-by-side placed antenna pairs. The overall isolation performance is then tuned by optimizing the shape and dimensions of this structure including cutting circular and rectangular slits from the resonant section.

The second major source of mutual coupling originates between orthogonal antenna pairs having a common edge. To address this source of mutual coupling an FSS based rectangular chained strip structure is introduced on both sides of the substrate. Finally, the antennas which are in back-to-back or across configuration are decoupled with the help of a meander line stub extended from ground planes with parasitic spiral strips in the gaps. A rectangular slit is added to show the connected ground also the proposed design shares a single/common ground as Fig. 2 shows the 3-D view in which all grounds are connected. The effect of this connected ground plane is clearly observed in Fig 6. and 7. The proposed three distinct decoupling structures for each of the configurations are illustrated in Fig. 3. All the dimensions for the proposed antenna and decoupling structures are listed in Table 1 and II respectively. The non-planar arrangement including non-connected grounds and shared ground plane configuration (SGP) and along with the finalized fabricated design is presented in Fig. 2

C. ANALYSIS AND OPTIMIZATION OF DECOUPLING

The analysis and optimization of the FSS based spiral enclosed meander line (SEM) and rectangular chained

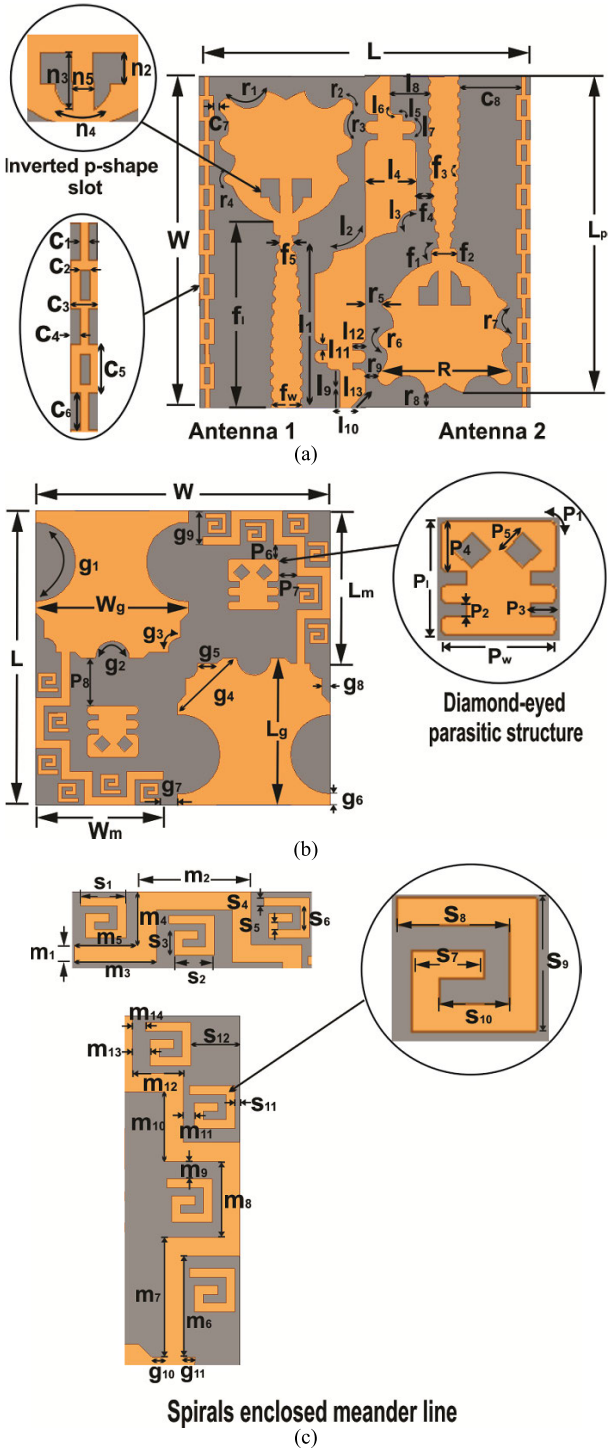

FIGURE 3. Geometrical configuration of antennas: (a) Top layer; (b) Bottom layer; (c) Spirals enclosed meander line decoupling structure.

decoupling structures are shown in Fig. 4(a) and (b) respectively. The analysis is performed by using a 3D full-wave electromagnetic simulator (Ansys HFSS). The SEM is simulated by placing it in an airbox with PEC and PMC boundary conditions along with the wave port excitation from orthogonal sides. However, the rectangular chain FSS structure is a periodic structure it is simulated with a one-dimensional

TABLE 1. Optimization of proposed antenna.

Para.	Value (mm)	Para.	Value (mm)	Para.	Value (mm)	Para.	Value (mm)
W	26	L_p	24.85	r_9	0.93	g_3	1.05
L	26	r_1	1.5	n_1	4	g_4	4
f_l	14.6	r_2	1.2	n_2	1.5	g_5	1.73
f_w	2.45	r_3	2	n_3	3	g_6	1
f_1	0.3	r_4	0.6	n_4	1.3	g_7	1.5
f_2	2	r_5	1.17	n_5	1	g_8	1.12
f_3	0.3	r_6	1.87	W_g	13.5	g_9	3.11
f_4	1.59	r_7	1.71	L_g	13	g_{10}	0.5
f_5	1.24	r_8	1.49	g_1	3.5	g_{11}	0.48
R	10.5			g_2	1.5		

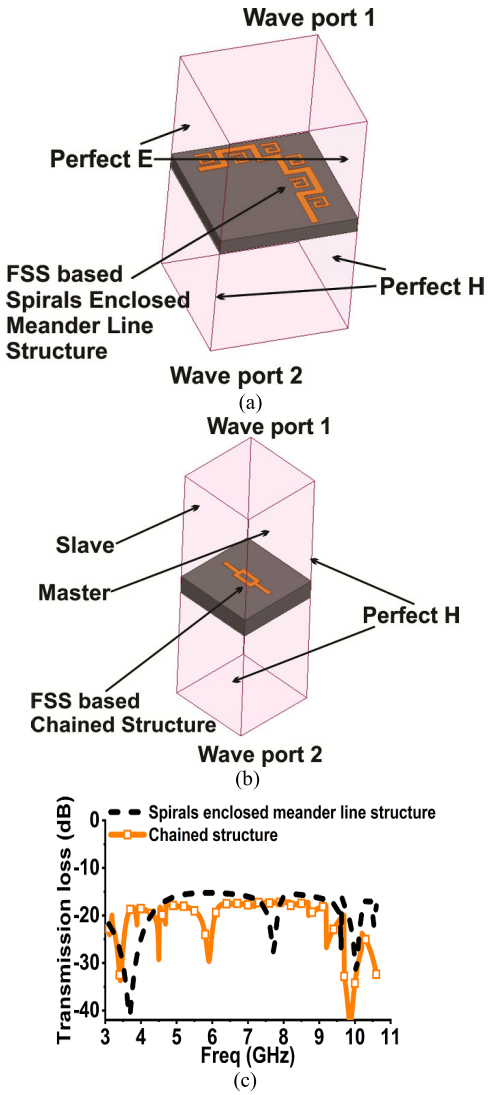

FIGURE 4. FSS analysis: (a) Analysis setup of SEM; (b) Analysis setup of chained structure; (c) Transmission loss.

periodic boundary condition as illustrated in Fig 4. These structures suppress transmission up to 20 dB enabling them

TABLE 2. Optimization of proposed decoupling structures.

Spirals enclosed meander line (SEM)				Chained structure, vertical strip and DES			
Para.	Value (mm)	Para.	Value (mm)	Para.	Value (mm)	Para.	Value (mm)
m_1	0.75	s_4	0.35	c_1	0.35	l_9	3
m_2	4.5	s_5	0.325	c_2	0.4	l_{10}	0.8
m_3	3.25	s_6	1	c_3	1.15	l_{11}	0.5
m_4	2.25	s_7	0.925	c_4	0.4	l_{12}	1
m_5	2.5	s_8	1.45	c_5	2	l_{13}	1.2
m_6	4	s_9	1.7	c_6	1.5	P_1	4.5
m_7	4.75	s_{10}	0.9	c_7	0.89	P_w	4.5
m_8	3	s_{11}	0.86	c_8	4.84	P_1	0.3
m_9	1.09	s_{12}	2.12	l_1	13.5	P_2	0.5
m_{10}	2.75			l_2	2.83	P_3	1
m_{11}	0.4			l_3	1.5	P_4	1.95
m_{12}	2			l_4	4	P_5	1
m_{13}	1.07			l_5	0.3	P_6	1.5
s_1	1.8			l_6	0.3	P_7	1.77
s_2	1.6			l_7	1	P_8	4.25
s_3	1.025			l_8	3.17		

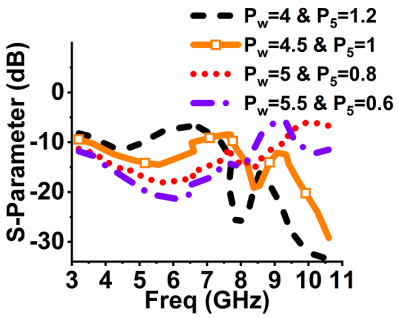

FIGURE 5. Parametric optimization of DES.

to be used as decoupling structures. Once these decoupling structures are introduced the impedance bandwidth is reduced as FSS based isolating structures are lossy in nature. Hence to enhance impedance bandwidth, compact parasitic elements are designed, optimized and introduced on the flip side of the substrate. These parasitic elements are referred to as diamond eyed structures (DES). It has rectangular slits on both sides. The dimensions of DES are also listed in Table 2.

D. PARAMETRIC OPTIMIZATION OF DES The FSS based isolating structures are lossy in nature and once these decoupling structures are introduced, the impedance bandwidth is reduced. Hence the DES structure is added to regain the bandwidth. The parametric analysis of the DES structure is given in Fig 5. Four combinations of 'P_w' and 'P_5' are simulated and presented in the figure, Overall, the optimized impedance matching over the whole band is achieved when $P_w = 4.5$mm and $P_5 = 1$mm. The rest of the parameters are also optimized through the EM simulator.

III. RESULTS AND DISCUSSIONS

Once the design optimization was completed through parametric analysis the structure was fabricated through a milling

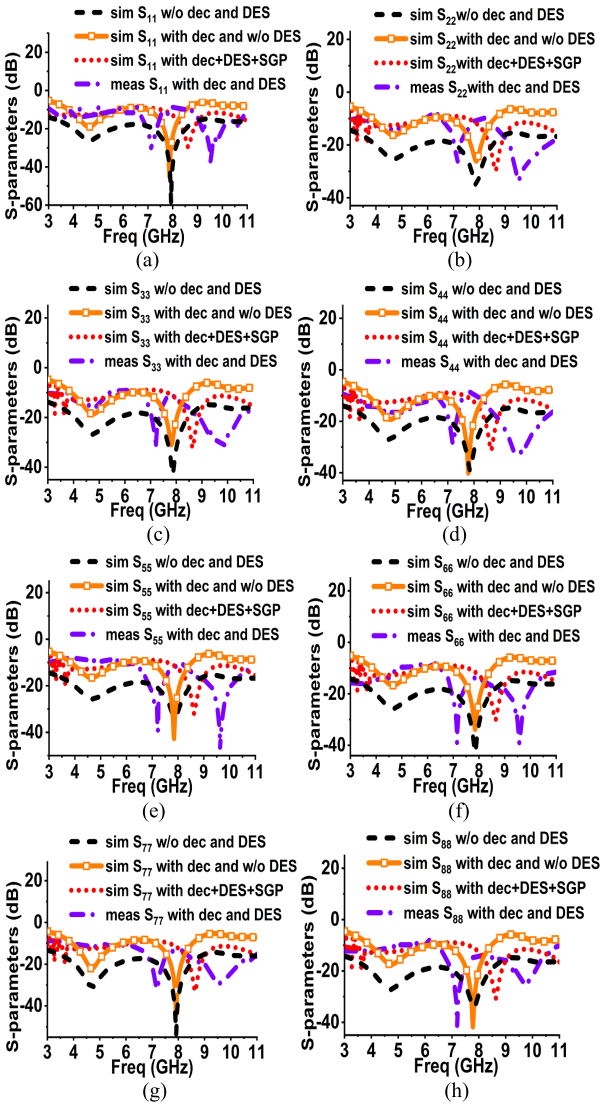

FIGURE 6. Simulated and measured S-parameters for; with and without decoupling, SGP and DES: (a)-(h) Antenna 1-8.

machine on a 1.6 mm thick FR 4 substrate. The antenna elements were arranged in a 3D configuration around a polystyrene foam and measured through a PNA-X (Agilent N5242A) network analyzer followed by radiation pattern measurement in a fully anechoic chamber. The results discussion is presented in the following subsections.

A. REFLECTION COEFFICIENT

The measured and simulated results of the S-parameter are presented in Fig. 6. The results reveal that the proposed system achieves more than 10 dB impedance bandwidth over the whole UWB band. Notably, improvement in impedance matching is observed at lower and prominently at higher frequencies when decoupling structures and DES are deployed alongside. The proposed DES has strong resonant characteristics at higher frequencies. While the polystyrene block is inserted to support the overall 3-D formation. More importantly, the antenna impedance performance with

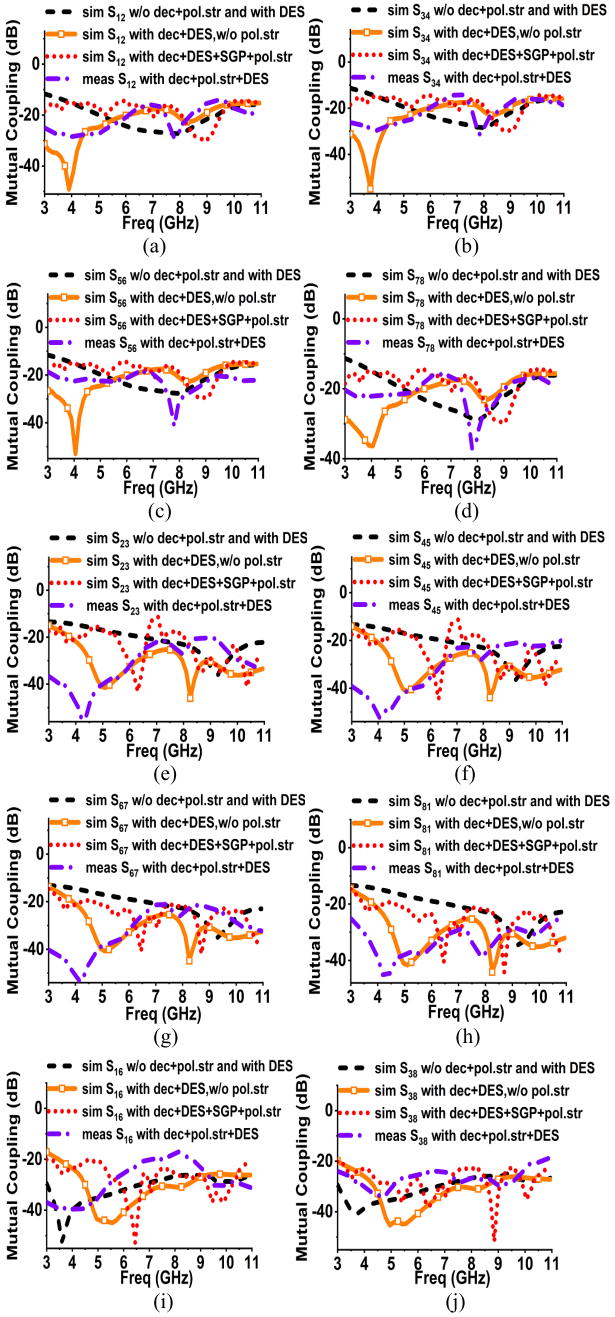

FIGURE 7. Simulated and measured mutual coupling for all configurations with and without decoupling, polystyrene, SGP and DES: (a)-(d) Side-by-side configuration; (e)-(h) Orthogonal configuration; (i)-(j) Across configuration.

SGP is also investigated. The results reveal that impedance matching at middle and higher frequencies tends to distort but remains within acceptable limits.

B. MUTUAL COUPLING

The proposed combination of isolation structures offers mutual coupling suppression amongst all combinations of the radiating elements. The graphs are reported for simulated and measured results with and without decoupling structures, polystyrene block and SGP. The side-by-side arrangement

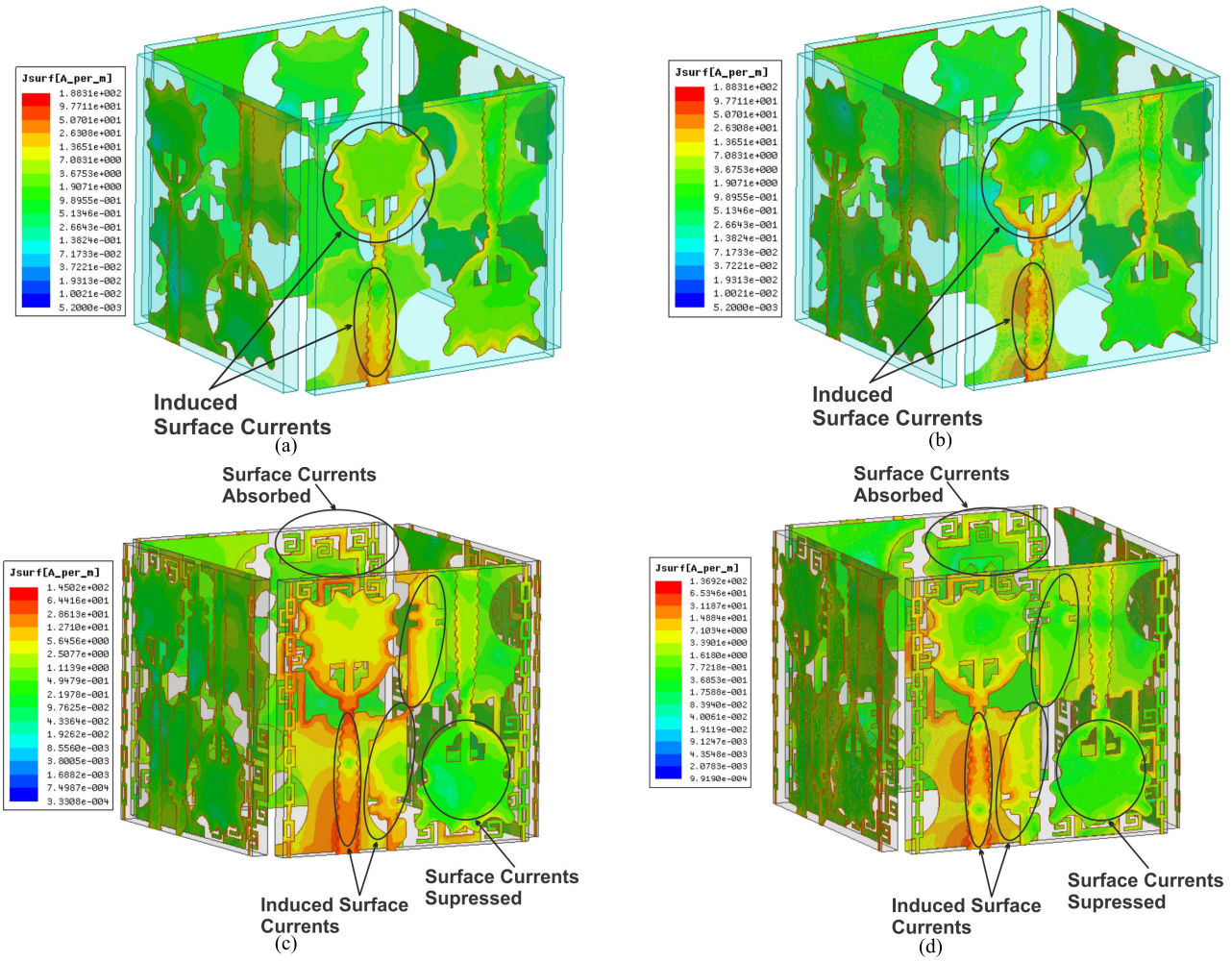

FIGURE 8. Surface current distribution: (a)-(b) at 4 and 10 GHz without decoupling; (c)-(d) at 4 and 10 GHz with decoupling.

of antenna pair on the substrate surface undergoes mutual coupling suppression of more than 20 dB with the help of transmission line resonator as shown in Fig. 7 (a)-(d). The FSS based rectangular chained strips and meander line with spirals achieve mutual coupling reduction of 22 dB and 30 dB over the whole band as depicted in Fig. 7 (e)-(h), and Fig. 7 (i)-(j) respectively. The enhanced isolation for the across configuration may be observed at lower frequencies owing to the intrinsic dielectric losses of polystyrene block. In addition to this, SGP configuration is also analyzed to check the performance of the proposed decoupling structures. It can be inferred from the results in Fig. 7 that, isolation performances of these structures are minimally affected owing to connected grounds. The isolation suppression of at least 16 dB, 17 dB and 22 dB is observed for side-by-side, orthogonal and across placed antennas. Overall, this SGP configuration undermines the isolation performance of the system by an average of 6 dB.

C. SURFACE CURRENT DISTRIBUTION

The surface current distribution with and without decoupling structure of the proposed antenna system is shown in Fig. 8. This distribution reveals that surface currents are induced at the feedline, ground plane, and vertical decoupling strip. Owing to very limited space constraints the vertical decoupling structures are optimized in such a way that they don't couple with the transmission line and the resonator. The suppression of surface currents can be observed at radiators and decoupling structures.

D. RADIATION CHARACTERISTICS

The E and H planes are shown in Fig. 9, both E and H plane results shown that the antenna is radiating in all directions owing to the omnidirectional nature of partial ground monopoles. The results showed some distortion as the proposed design is non-planar. Moreover, fabrication imperfections lead to some extent of pattern distortion.

E. MIMO PERFORMANCE PARAMETERS

The diversity performance of the proposed MIMO system is investigated by calculating various MIMO parameters i.e. Envelope Correlation Coefficient (ECC), Channel Capacity Loss (CCL), Total Active Reflection Coefficient (TARC), Directivity Gain (DG), and Mean Effective Gain (MEG).

TABLE 3. Comparison with existing work.

Ref. No	Size (mm^2)	Antenna arrangement	Ports	Isolation (dB)	ECC (mag)/dB	CCL (bits/s/Hz)	TARC (dB)	DG (dB)	MEG (dB)	Freq. band (GHz)
[17]	40 × 35 Non planar	Orthogonal	2	20	-40 dB	0.5	0.45	-	-	3.1-10.6
[26]	34×36 Non-planar	Orthogonal and across	4	20	<0.005	<0.4	< -4	-	-	3.1-10.6
[27]	50×50 Non-planar	Side-by-side and orthogonal	8	20	<0.5	-	-	-	-	3-11
[28]	28×23 Non-planar	Across and diagonal	8	20	<0.0025	0.35	-11	-	-	3-11
[29]	85×85	Orthogonal	8	< 15	<0.2	-	<0	-	-	3.1-10.6
[30]	120×70	Side-by-side	10	18	<0.21	-	-	-	-	3.2 – 6.1
[31]	150×85	Side-by-side	2	< 30	0.06	-	-	-	-	4.6-5.8
This work	**26×26**	**Side-by-side, orthogonal and across**	**8**	**> 20, 22 and 30.**	**<0.08**	**<0.35**	**< -12**	**>9.96**	**< 3**	**3-11**

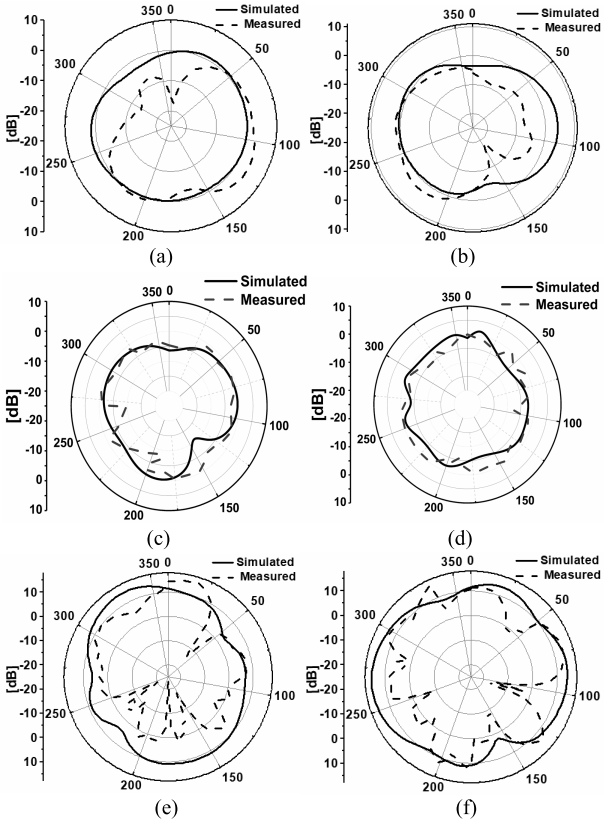

FIGURE 9. Radiation patterns: (a),(c), (e) E-plane at 4 GHz, 7 GHz and 10 GHz; (b), (d), (f) H-plane at 4 GHz, 7 GHz and 10 GHz.

ECC and CCL should be less than 0.5, TARC, DG, and MEG should be less than 0 dB, 9-10 dB, and 3dB respectively [20]. The general formulas for these parameters are expressed in (1), (2), (3), (4), and (5) [21]–[25].

$$\rho_e = \frac{\left|\iint_{4\pi}\left[\vec{E}_i(\theta,\phi)\times\vec{E}_j(\theta,\phi)\right]d\Omega\right|^2}{\iint_{4\pi}\left|\vec{E}_i(\theta,\varphi)\right|^2 d\Omega \iint_{4\pi}\left|\vec{E}_j(\theta,\varphi)\right|^2 d\Omega}. \quad (1)$$

$$C_{(loss)} = -log_2(det\psi^R), \quad (2)$$

where,

$$\psi^R = \begin{bmatrix}\rho_{11} & \rho_{12}\\ \rho_{21} & \rho_{22}\end{bmatrix}, \quad \rho_{ii} = 1 - \left(|S_{ii}|^2 + |S_{ij}|^2\right)$$

and

$$\rho_{ij} = -\left(S_{ii}^* S_{ij} + S_{ji}^* S_{ij}\right) for i, j = 1 \text{ or } 2.$$

$$TARC = \sqrt{\frac{\left|\sum_{n=8} S_{1n}\right|^2 + \ldots + \left|\sum_{n=8} S_{8n}\right|^2}{8}}. \quad (3)$$

$$DG = 10\sqrt{1 - |\rho_e|^2}. \quad (4)$$

$$MEG_{ithport} = 0.5\left(1 - \sum_{i=portnumber}^{N=numberofantennas} |S_{ij}|^2\right). \quad (5)$$

For the proposed MIMO antenna system each parameter is calculated for all configurations including side-by-side, orthogonal, and across are shown in Fig. 10. Overall the proposed design achieved ECC < 0.08, CCL < 0.35, TARC < −12 dB, DG > 9.88 dB and MEG < 3dB in all configuration as shown in Fig. 10 (a)-(e). s

IV. COMPARISON WITH EXISTING WORK

Several UWB-MIMO antenna systems are reported in the literature. However, the proposed MIMO system is compact, provides improved isolation, and flexibility of configurations. This non-planar system consists of 8-antenna elements in a

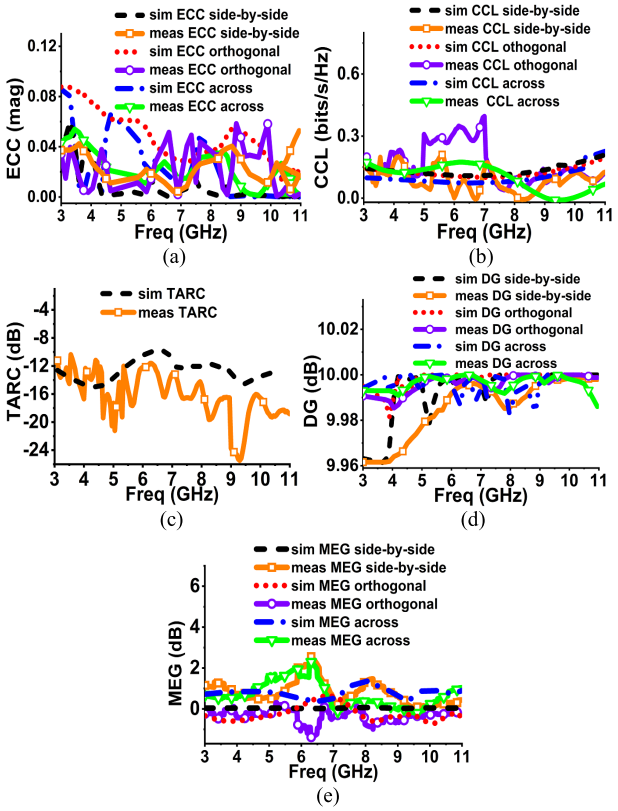

FIGURE 10. MIMO performance parameters: (a) ECC; (b) CCL; (c) TARC; (d) DG; (e) MEG.

cuboidal form suitable for high bandwidth system-in-package applications with a small footprint that is highly competitive as compared to the existing both planar and non-planar designs. Additionally, the performance parameters are in a well acceptable range. A detailed comparison with the existing work is listed in Table 3.

V. CONCLUSION

In this work, a compact and non-planar 8-element UWB MIMO antenna system is presented. This system assures its suitability for 3D system-in-package applications owing to a compact non-planar arrangement. The designing approach leads to antenna configuration by applying several techniques including but are not limited to beveling, chamfering, defected ground structures and, parasitic structures. Moreover, three distinct isolation mechanisms are developed to isolate the proposed configurations. The isolation mechanism mainly involves an FSS based analysis and approach to strengthen the isolation in this proximity system. Vertical strip rectangular chained strips, FSS employed meander line with spirals decoupling structure achieves overall isolation of not less than 20 dB and as high as 30 dB. Yet to improve and regain the impedance, DES is implemented as a parasitic structure. Notably, improved MIMO performance parameters prove this system relevance for portable communication devices for UWB applications.

ACKNOWLEDGMENT

The authors are thankful to the Chief Minister Delivery Unit (CMDU) Balochistan, for sharing their resources for simulations and providing technical support.

REFERENCES

[1] S. Zhang, P. Zetterberg, and S. He, "Printed MIMO antenna system of four closely-spaced elements with large bandwidth and high isolation," *Electron. Lett.*, vol. 46, no. 15, pp. 1052–1053, Jul. 2010.

[2] I. Gresham, A. Jenkins, R. Egri, C. Eswarappa, N. Kinayman, N. Jain, R. Anderson, F. Kolak, R. Wohlert, S. P. Bawell, J. Bennett, and J.-P. Lanteri, "Ultra-wideband radar sensors for short-range vehicular applications," *IEEE Trans. Microw. Theory Techn.*, vol. 52, no. 9, pp. 2105–2122, Sep. 2004.

[3] J. Wang, L. Zhang, Q. Wang, L. Chen, J. Shi, X. Chen, Z. Li, and D. Shen, "Multi-class ASD classification based on functional connectivity and functional correlation tensor via multi-source domain adaptation and multi-view sparse representation," *IEEE Trans. Med. Imag.*, vol. 39, no. 10, pp. 3137–3147, Oct. 2020.

[4] B. H. Wang, H. T. Hui, and M. S. Leong, "Global and fast receiver antenna selection for MIMO systems," *IEEE Trans. Commun.*, vol. 58, no. 9, pp. 2505–2510, Sep. 2010.

[5] D. Sipal, M. P. Abegaonkar, and S. K. Koul, "Easily extendable compact planar UWB MIMO antenna array," *IEEE Antennas Wireless Propag. Lett.*, vol. 16, pp. 2328–2331, 2017.

[6] L. Wu, Y. Xia, X. Cao, and Z. Xu, "A miniaturized UWB-MIMO antenna with quadruple band-notched characteristics," *Int. J. Microw. Wireless Technol.*, vol. 10, no. 8, pp. 948–955, Oct. 2018.

[7] R. Chandel, A. K. Gautam, and K. Rambabu, "Design and packaging of an eye-shaped multiple-input–multiple-output antenna with high isolation for wireless UWB applications," *IEEE Trans. Compon., Packag., Manuf. Technol.*, vol. 8, no. 4, pp. 635–642, Apr. 2018.

[8] M. A. Ul Haq and S. Koziel, "Ground plane alterations for design of high-isolation compact wideband MIMO antenna," *IEEE Access*, vol. 6, pp. 48978–48983, 2018.

[9] Z. Tang, X. Wu, J. Zhan, S. Hu, Z. Xi, and Y. Liu, "Compact UWB-MIMO antenna with high isolation and triple band-notched characteristics," *IEEE Access*, vol. 7, pp. 19856–19865, 2019.

[10] M. Bilal, R. Saleem, M. F. Shafique, and H. A. Khan, "MIMO application UWB antenna doublet incorporating a sinusoidal decoupling structure," *Microw. Opt. Technol. Lett.*, vol. 56, no. 7, pp. 1547–1553, Jul. 2014.

[11] W. Youcheng, Y. Yanjiao, C. Qingxi, and P. Hucheng, "Design of a compact ultra-wideband MIMO antenna," *J. Eng.*, vol. 2019, no. 20, pp. 6487–6489, 2019.

[12] L. Wang, Z. Du, H. Yang, R. Ma, Y. Zhao, X. Cui, and X. Xi, "Compact UWB MIMO antenna with high isolation using fence-type decoupling structure," *IEEE Antennas Wireless Propag. Lett.*, vol. 18, no. 8, pp. 1641–1645, Aug. 2019.

[13] Z. Li, C. Yin, and X. Zhu, "Compact UWB MIMO vivaldi antenna with dual band-notched characteristics," *IEEE Access*, vol. 7, pp. 38696–38701, 2019.

[14] P. Kumar, S. Urooj, and A. Malibari, "Design of quad-port ultra-wideband multiple-input-multiple-output antenna with wide axial-ratio bandwidth," *Sensors*, vol. 20, no. 4, p. 1174, Feb. 2020.

[15] P. Kumar, S. Urooj, and F. Alrowais, "Design of quad-port MIMO/Diversity antenna with triple-band elimination characteristics for super-wideband applications," *Sensors*, vol. 20, no. 3, p. 624, Jan. 2020.

[16] A. Shaikh, R. Saleem, M. F. Shafique, and A. K. Brown, "Reconfigurable dual-port UWB diversity antenna with high port isolation," *Electron. Lett.*, vol. 50, no. 11, pp. 786–788, May 2014.

[17] S. I. Jafri, R. Saleem, M. F. Shafique, and A. K. Brown, "Compact reconfigurable multiple-input-multiple-output antenna for ultra wideband applications," *IET Microw., Antennas Propag.*, vol. 10, no. 4, pp. 413–419, Mar. 2016.

[18] M. Bilal, K. Khalil, R. Saleem, F. A. Tahir, and M. F. Shafique, "An interdigital FSS based dual channel UWB-MIMO antenna array for system-inpackage applications," *Appl. Comput. Electromagn. Soc. J.*, vol. 32, no. 3, pp. 203–208, 2017.

[19] E. Hammerstad and O. Jensen, "Accurate models for microstrip computer-aided design," in *IEEE MTT-S Int. Microw. Symp. Dig.*, May 1980, pp. 407–409.

[20] E. Thakur, N. Jaglan, and S. D. Gupta, "Design of compact UWB MIMO antenna with enhanced bandwidth," *Prog. Electromagn. Res. C*, vol. 97, pp. 83–94, 2019.
[21] Z. Wang, C. Li, Q. Wu, and Y. Yin, "A metasurface-based low-profile array decoupling technology to enhance isolation in MIMO antenna systems," *IEEE Access*, vol. 8, pp. 125565–125575, 2020.
[22] H. Shin and J. Hong Lee, "Capacity of multiple-antenna fading channels: Spatial fading correlation, double scattering, and keyhole," *IEEE Trans. Inf. Theory*, vol. 49, no. 10, pp. 2636–2647, Oct. 2003.
[23] N. Jaglan and S. D. Gupta, "Design and analysis of performance enhanced microstrip patch antenna with EBG substrate," *Int. J. Microw. Opt. Technol.*, vol. 10, no. 2, pp. 79–88, 2015.
[24] M. M. Bait-Suwailam, M. S. Boybay, and O. M. Ramahi, "Electromagnetic coupling reduction in high-profile monopole antennas using single-negative magnetic metamaterials for MIMO applications," *IEEE Trans. Antennas Propag.*, vol. 58, no. 9, pp. 2894–2902, Sep. 2010.
[25] A. A. Glazunov, A. F. Molisch, and F. Tufvesson, "Mean effective gain of antennas in a wireless channel," *IET Microw., Antennas Propag.*, vol. 3, no. 2, pp. 214–227, Mar. 2009.
[26] M. Bilal, R. Saleem, H. H. Abbasi, M. F. Shafique, and A. K. Brown, "An FSS-based nonplanar quad-element UWB-MIMO antenna system," *IEEE Antennas Wireless Propag. Lett.*, vol. 16, pp. 987–990, 2017.
[27] M. S. Khan, F. Rigobello, B. Ijaz, E. Autizi, A. D. Capobianco, R. Shubair, and S. A. Khan, "Compact 3-D eight elements UWB-MIMO array," *Microw. Opt. Technol. Lett.*, vol. 60, no. 8, pp. 1967–1971, Aug. 2018.
[28] T. Shabbir, R. Saleem, S. S. Al-Bawri, M. F. Shafique, and M. T. Islam, "Eight-port metamaterial loaded UWB-MIMO antenna system for 3D system-in-package applications," *IEEE Access*, vol. 8, pp. 106982–106992, 2020.
[29] R. Mathur and S. Dwari, "8-port multibeam planar UWB-MIMO antenna with pattern and polarisation diversity," *IET Microw., Antennas Propag.*, vol. 13, no. 13, pp. 2297–2302, Oct. 2019.
[30] A. Singh and C. E. Saavedra, "Wide-bandwidth inverted-F stub fed hybrid loop antenna for 5G sub 6 GHz massive MIMO enabled handsets," *IET Microw., Antennas Propag.*, vol. 14, no. 7, pp. 677–683, Jun. 2020.
[31] J. Zhang, S. Yan, X. Hu, and G. A. E. Vandenbosch, "Mutual coupling suppression for on-body multiantenna systems," *IEEE Trans. Electromagn. Compat.*, vol. 62, no. 4, pp. 1045–1054, Aug. 2020.

SANIA SHAKIR received the B.S. degree in telecommunication engineering from the Balochistan University of Information Technology, Engineering and Management Sciences (BUITEMS), Quetta, Pakistan, in 2015, and the master's degree in telecommunication engineering from BUITEMS. Her main research interests include the UWB-MIMO antenna systems and frequency selective surfaces.

MUHAMMAD BILAL received the B.S. degree in telecommunication engineering from the Balochistan University of Information Technology, Engineering and Management Sciences (BUITEMS), Quetta, Pakistan, in 2011, and the master's degree in telecommunication engineering and the Ph.D. degree in antennas and electromagnetics from the University of Engineering and Technology (UET) Taxila, Pakistan, in 2014, and 2018, respectively. Since February 2018, he has been an Assistant Professor with the Department of Telecommunication Engineering, BUITEMS, where he is heading the Higher Education Commission (HEC) funded research project while supervising graduate and post-graduate students. He has published in many reputable scientific journals and conferences. His current research interests include UWB-MIMO systems, high-gain portable devices, frequency selective surfaces, and reflectarrays.

SYED MUZAHIR ABBAS (Senior Member, IEEE) received the B.Sc. degree in electrical (telecommunication) engineering from the COMSATS Institute of Information Technology (CIIT), Islamabad, Pakistan, in 2006, the M.Sc. degree in computer engineering from the Center for Advanced Studies in Engineering (CASE), Islamabad, in 2009, and the Ph.D. degree in electronics engineering from Macquarie University, North Ryde, NSW, Australia, in 2016. He has been a Transmission Engineer with Alcatel-Lucent, Pakistan; an RF Engineer with CommScope, Australia; a Senior Antenna Design Engineer with Benelec Technologies, Australia; and a Visiting Researcher with the ElectroScience Laboratory, The Ohio State University, USA, and the Queen Mary University of London, U.K. He has lectured various courses at CIIT; Western Sydney University, Australia; Macquarie University, Australia; and The University of Sydney, Australia. He is currently working as a Senior Principal Engineer with Benelec Technologies. His research interests include base station antennas, mmWave antennas, high-impedance surfaces, frequency selective surfaces, flexible/embroidered antennas, CNT yarns, CNT/graphene-based antennas, reconfigurable antennas/electronics, and the development of antennas for UWB and WBAN applications. He has received several prestigious awards and fellowships, including the 2020 IEEE 5G World Forum Best Paper Award, the 2019 IEEE NSW Outstanding Young Professional Award, the 2018 Young Scientist Award (Commission B—Field and Waves) from the International Union of Radio Science (URSI), the 2013 CSIRO Postgraduate Fellowship, the 2012 iMQRES Award for Ph.D., and the Research Productivity Award, in 2012 and 2010, from CIIT.

NOMAN SALEEM received the M.S. degree in information technology from Balochistan University of Information Technology, Engineering and Management Sciences (BUITEMS). Since July 2018, he has been an Assistant Director MIS with the Chief Minister Delivery Unit, Pakistan, where he is supervising intra and inter provincial research and development activities. He is currently managing linkage and funding between degree awarding institutions and industries focusing on antennas design and manufacturing. His work on E-Governance, file tracking system, COVID-19 trend monitoring and activity tracking system of Balochistan are widely recognized and honored provincially.

ZAHID RAUF (Member, IEEE) received the B.E. degree in information technology from Hamdard University, Islamabad, Pakistan, the M.Sc. degree in electrical and electronic engineering from the University of Leeds, U.K., and the Ph.D. degree in electrical and electronic engineering from the University of Canterbury, New Zealand, in 2013. He is currently serving as an Associate Professor with the Department of Electrical Engineering and the Dean of graduate studies with the Balochistan University of Information Technology, Engineering and Management Sciences (BUITEMS), Quetta, Pakistan. His research interests include digital wireless communications, including massive MIMO, multiuser communication systems, channel estimation, equalization and low complexity iterative detection algorithms, cooperative relaying networks, optimal and adaptive resource allocation in wireless networks, and cross-layer design and analysis (primarily physical and link layer).

RAJA ASIF WAGAN received the bachelor's degree in computer science from the University of Sindh, Pakistan, in 2005, the master's degree in information technology from Universiti Utara Malaysia, and the Ph.D. degree in information and communication engineering from Harbin Engineering University, Harbin, China. He is currently serving as an Assistant Professor with the Department of IT, Balochistan University of Information Technology, Engineering and Management Sciences (BUITEMS), Pakistan. His research interests include routing protocols, wireless sensor networks, and computer networks.

RASHID SALEEM received the B.S. degree in electronic engineering from the Ghulam Ishaq Khan Institute of Engineering Sciences and Technology, Pakistan, in 1999, the M.S. degree from the University of Engineering and Technology (UET) Taxila, Pakistan, through the Center for Advanced Studies in Engineering, Pakistan, in 2006, and the Ph.D. degree from The University of Manchester, U.K., in 2011. He pursued a career in the telecommunication industry for several years while continuing education. He worked on antennas, channel modeling, and interference aspects of ultra wideband systems during his Ph.D., and was a member of a team designing and testing arrays for the Square Kilometer Array Project. He is currently working as an Assistant Professor with UET Taxila, where he is supervising several postgraduate students and heading the Microwave Antennas and Propagation (MAP) Research Group. His research interests include antennas, angle-of-arrival-based channel modeling, microwave periodic structures, and metamaterial.

MUHAMMAD FARHAN SHAFIQUE (Senior Member, IEEE) received the B.Eng. degree from Hamdard University, Karachi, Pakistan, in 2003, the M.S. degree from the University of Paris-Est Marne-La-Vallee, Paris, France, in 2005, and the Ph.D. degree in electronic and communications engineering from the University of Leeds, Leeds, U.K., in 2010. From 2007 to 2010, he was involved in establishing the LTCC fabrication facility at the Institute of Microwave and Photonics, University of Leeds. He is currently working as an Associate Professor with COMSATS University Islamabad (CUI), Pakistan. He is also the Founding Head of the MCAD Research Group and the Associate Director of the Center for Advanced Studies in Telecommunications. He has extensive experience of laser micromachining and multilayer LTCC device modeling and fabrication. His research interests include multilayered-microwave device fabrication on LTCC and thick-film technology, RF antenna and antenna arrays, ultra wideband diversity antennas, and MEMS packaging. He is also involved in dielectric characterization of materials using microwave techniques and fabrication of ceramic microfluidic devices.